Climate change more than doubled the likelihood of extreme fire weather conditions in Eastern Canada

Authors

1. Clair Barnes, *Grantham Institute, Imperial College London, UK*
2. Yan Boulanger, *Canadian forest service, Natural Resources Canada*
3. Theo Keeping, *Leverhulme Centre for Wildfires, Environment and Society, Imperial College London & University of Reading*
4. Philippe Gachon, *Université du Québec à Montréal*
5. Nathan Gillett, *Canadian Centre for Climate Modelling and Analysis, Environment and Climate Change Canada*
6. Jonathan Boucher, *Canadian Forest Service, Natural Resources Canada*
7. François Roberge, *Université du Québec à Montréal*
8. Sarah Kew, *Royal Netherlands Meteorological Institute (KNMI), De Bilt, The Netherlands*
9. Olivia Haas, *Leverhulme Centre for Wildfires, Environment and Society and Georgina Mace Centre for the Living Planet, Imperial College London*
10. Dorothy Heinrich, *Red Cross Red Crescent Climate Centre, The Hague, the Netherlands*
11. Maja Vahlberg, *Red Cross Red Crescent Climate Centre, The Hague, the Netherlands*
12. Roop Singh, *Red Cross Red Crescent Climate Centre, The Hague, the Netherlands*
13. Manon Elbe, *Red Cross Red Crescent Climate Centre, The Hague, the Netherlands*
14. Sajanika Sivanu, *Red Cross Red Crescent Climate Centre, The Hague, the Netherlands*
15. Julie Arrighi, *Red Cross Red Crescent Climate Centre, The Hague, the Netherlands*
16. Maarten van Aalst, *Royal Netherlands Meteorological Institute (KNMI), De Bilt, The Netherlands*
17. Fredi Otto, *Grantham Institute, Imperial College London, UK*

Review authors

1. Mariam Zachariah, *Grantham Institute, Imperial College London, UK*
2. Folmer Krikken, *Weather Trade Net*
3. Xianli Wang, *Canadian forest service, Natural Resources Canada*
4. Sandy Erni, *Natural Resources Canada (Vulnerability and exposure)*
5. Emily Pietropalo, *Canadian Red Cross (Vulnerability and exposure)*
6. Amy Avis, *Canadian Red Cross (Vulnerability and exposure)*
7. Alexandrine Bisaillon, *Ouranos, Canada (Vulnerability and exposure)*
8. Joyce Kimutai, *Grantham Institute, Imperial College London, UK*

Main findings

- Fire weather is one important condition driving wildfires, although changes in vegetation (wildfire fuel), ignition factors, and fire management strategies also contribute to future wildfire risk.
- In today's climate, intense fire weather like that observed in May-July 2023 is a moderately extreme event, expected to occur once every 20-25 years. This means in any given year such an event is expected with 4-5% probability.
- Climate change made the cumulative severity of Québec's 2023 fire season
- to the end of July around 50% more intense, and seasons of this severity at least seven times more likely to occur. Peak fire weather (FWI7x) like that experienced this year is at least twice as likely, and the intensity has increased by about 20% due to human-induced climate change.
- Observed changes are typically larger than in the models.
- As expected, likelihood and intensity are projected to increase further in a 2°C warmer world.
- Changes in fire weather are associated with an increase in temperature and decrease in humidity, both of which are driven by human-induced warming; the effect was compounded in 2023 by unusually low precipitation
- The extent, magnitude, and location of concomitant wildfires posed significant challenges for wildfire management which largely focused on disaster response and wildfire containment to limit the impact on lives and infrastructure.
- The wildfires had disproportionate impacts on indigenous, fly-in, and other remote communities who were particularly vulnerable due to lack of services and barriers to response interventions.
- The consequences from the wildfires reached far beyond the burned areas with displaced impacts due to air pollution threatening health, mobility, and economic activities of people across North America.
- As fire weather risks increase, changes in fire management strategies and increased resources will be required to meet the increased challenges.

1 Introduction

From May to July 2023, Canada witnessed exceptionally extreme fire-weather conditions. The event was caused by record warm temperatures and persistent and spatially extensive drought conditions throughout most of the country during that time period (ESCER 2023). These very fire-conducive conditions fueled intense and extensive wildfires that burned more than 13.1 million hectares (Mha) (as of August 3rd) of forests in the country (Canadian Interagency Forest Fire Centre (CIFFC), 2023). Such an area burned represents by far the worst fire season in recent history even though the May-July period only spans approximately half of the typical fire season.

Wildfires are a common phenomenon within Canadian forests. On average, wildfires burn 2.5 Mha annually in the country although there is strong interannual variability. Most of the area burned is caused by large lightning-caused fires (Stocks et al., 2002). The typical fire season stretches from April to October with the most active period spanning between June and August. These natural disturbances are an essential component of many Canadian ecosystems, with several processes dependent on (e.g., tree species regeneration) or highly impacted by them (e.g., carbon cycling).

This year's fire season in Canada is exceptional in many aspects. As of August 16th, more than 5700 fires have burned 13.7 Mha since the beginning of the fire season (CIFFC, 2023), already exceeding the previous record set in 1989 when 7.6 Mha burned for the whole season (Canadian National Fire Database 2023). Since May, area burned is accumulating at a record pace, with virtually no respite at the national level (Canadian Wildland Fire Information System (CWFIS), 2023). Unlike other active fire seasons in Canada, this year's fire activity is spatially extensive, with intense fire activity stretching nationwide, from the Pacific to the Atlantic oceans. By August 16th, the provinces of Alberta (1.9 Mha), Québec (5.3 Mha), Nova Scotia (25 thousand hectares - hereafter, 25 kha) and British Columbia (1.6 Mha) had already seen their most active fire season since records began. These conditions fueled 29 mega-fires (>100 kha) by mid July, breaking the previous record 17 in 1989, with four fires reaching >500 kha, including one fire in northern Québec reaching >1.2 Mha (from SOPFEU data on August 3rd). As a consequence, these four fires are among the ten biggest wildfires in Canada since 1950 (Canadian National Fire Database 2023). Such record fire activity prompted the Canadian Interagency Forest Fire Centre (CIFFC) to declare the national preparedness level 5 on May 11th as fire fighting resource demands were extreme in many provinces, prompting limited national availability and commanding the mobilisation of a record number of international resources. Dangerous fires burning close to communities or excessively bad air quality led to the highest number of fire-related evacuees since at least 1980 (Beverly and Bothwell, 2011; Canadian Forest Service, 2023), impacting Indigenous communities in particular. On May 28th, extreme fire conditions within the wildland urban interface led to the destruction of at least 150 buildings in Tantallon, a suburb of Halifax, Nova Scotia, making it one of the most catastrophic wildfire-related events in recent Canadian history. In Québec, fires caused numerous power outages in urban centres including Montreal (La Presse, 2023).

Extreme wildfire conditions in Canada have been fueled by intense, spatially extensive and persistent fire-conducive weather conditions across the country since the beginning of May. Canada experienced its warmest May-July period since 1940, beating the previous record set in 1998 by a huge margin (0.8C). More specifically in May, a huge swath of central, western and northern Canada experienced their warmest May on record. At the national scale, relative humidity tied its second lowest value, while snow water equivalent was second lowest since 1950 (based on ERA5 reanalysis). During that month, warm, dry and continuous southeast flow conditions associated with high 500 hPa geopotential height anomalies fueled extensive fire spread in Alberta, Northern British Columbia, central Saskatchewan and southwestern portions of the Northwest Territories. In particular, an intense 7-day heatwave occurred at the beginning of May in Alberta, followed by further heatwaves in the middle of the month. Although fires are a common occurrence in Alberta in May (Parisien et al., 2023), fire spread this early in the season in the Northwest Territories is rather uncommon, with fire activity more typically recorded between June and August (Canadian National Fire Database 2023). At the end of the month, Nova Scotia, a maritime province in eastern Canada that is not used to seeing high levels of fire activity, experienced its largest fire on record, which burned more than 20 kha. By the end of the month, 2.8 Mha (as assessed from remote imagery hot spots) had already burned nationally, easily surpassing the 30-yr average for the whole fire season (Stocks et al., 2002).

Canada also experienced its warmest June on record in terms of both maximum and mean daily temperatures, and also its driest in terms of relative humidity (ESCER, 2023). As a result, all components (except for the initial spread index which ranked 3rd since 1950) of the fire-weather index, when averaged at the national scale, set record values and sometimes by huge margins, especially for indices measuring medium to long-term drought conditions (i.e., the duff moisture code, the drought code and the build-up index). Concomitantly, warm and dry conditions that developed in early May persisted through June in eastern Canada. On June 1st, atmospheric convection triggered the formation of several isolated thunderstorms and lightning that led to the ignition of more than 120 fires, mostly throughout the southern tier and the northwest portions of the province of Québec. On-going drought conditions supported by several short impulses of warm, dry and windy conditions during the following weeks prompted huge fire growth within both the extensive (EPZ) and intensive fire protection zones (IPZ) of Québec (SOPFEU). These conditions led to the largest ever observed fire within both the IPZ (460 kha) and the EPZ (1.1 Mha). Total area burned within the IPZ (1.5 Mha as of July 10th 2023) has surpassed the previous record set in 1923 (1.2 Mha). In this latter zone, more area burned between June 1st and June 25th (1.128 Mha) than the previous 20 years combined (1.121 Mha, SOPFEU). Persistent drought conditions in June within several portions of the country allow for continuous burning of fires ignited in May, with several still out-of-control at the time of writing (August 16th). Dense smoke plumes originating from these fires prompted air quality alerts/warnings for large portions of the densely populated both in Canada and northern United States during several days. Furthermore, smoke plumes travelled the Atlantic causing hazy skies in western Europe. Classes were suspended and schools closed across both Canada and the United States, such as in Nova Scotia (Nova Scotia, 2023), New York (The New York Times, 2023), New Jersey (CBS News, 2023), and Connecticut (CT Insider, 2023).

Although the extent of the impacts of this year's fires are yet to be thoroughly assessed in the province, no doubt that these will be substantial in both the short- and long terms. In the short term, a large swath of the burned commercial forest might have to be replanted at high cost as the result of potential extensive regeneration failures. Salvage logging (Leduc et al., 2015) will also have to be conducted in burned stands containing harvestable timber following the province's special management plans. In the medium- and long-term, annual allowable cut might have to be reviewed downward to take into account this year's wildfire impacts on forest stand age structure. In addition, this year's wildfires could substantially impact Canada's forest carbon balance (Kurz et al., 2009), alter biodiversity attributes through spatially extensive changes in forest landscape composition and structure (Leblond et al., 2022; Drapeau et al., 2000; Bergeron et al., 2017) and affect Indigenous traditional territories (Belisle, 2022).

Weather and climate conditions strongly impact wildfire characteristics at several temporal and spatial scales, with warmer, drier and windier conditions all increasing the likelihood that wildfires will ignite, spread, and intensify (Moritz et al., 2005). For instance, paleoecological studies have concluded that for each degree Celsius of warming, fire size triples in boreal Canada (Ali et al., 2012). Warmer temperatures over the last decades (Bush and Lemmen 2019) have led to a lengthening of the fire season as well as the occurrence of more severe and more frequent fire-prone weather conditions (Jain et al., 2015, 2022; Abatzoglu et al., 2018, Hicke et al., 2022). These in turn substantially reduce vegetation moisture content over a longer time period during the year, increasing fuel flammability (Ellis et al., 2022), fire ignition potential as well as severely altering fire behaviour and severity. In these northern ecosystems, such trends are most important within the boreal forest where significant increases in annual area burned and in large fire size have occurred since the middle of the 20th century (Hanes et al., 2019), mostly as the result of warmer temperatures (Gillett et al., 2004). Increased anthropogenic climate forcing have also made fire-weather conditions leading to mega-fires (Kirchmeier-Young et al., 2017; Zhang et al., 2019), record-breaking fire seasons (Kirchmeier-Young et al., 2018) and extreme synoptic-scale fire-prone conditions (Philip et al., 2022) much more likely in Canada. Since 1959, average annual area burned has more than doubled, increasing at a rate of 300 Kha per decade (Hanes et al., 2019). As a result, the financial burden associated with fire management and suppression in Canada is also trending upward, with annual costs increasing by 120M$ per decade (2009 constant CAN$) since 1970 (Hope et al., 2016). Based on these and other studies the IPCC assessed with medium confidence that anthropogenic climate change has increased the area burned by wildfires in western North America (Hicke et al., 2022). Future anthropogenic warming would further increase the severity and occurrence of fire-prone weather conditions in Canada, leading to substantial increases in e.g., annual area burned (Boulanger et al., 2014; Zhang et al., 2019). Over eastern Canada, forest fires are also strongly sensitive to changes in atmospheric and oceanic conditions over the North Atlantic, as high intensity of the fire weather index (FWI) in Québec occurs more often during seasons with negative North Atlantic Oscillation (NAO), blocking events, and/or with positive anomalies in sea surface temperatures over this oceanic basin (Wazneh et al., 2021). The impact from the blocking event over both the North Atlantic and Hudson Bay areas at the end of May and over much of June 2023 was additionally exacerbated by very dry conditions in much of Québec, in particular in the north, where the fourth largest precipitation deficit since 1950 was observed.

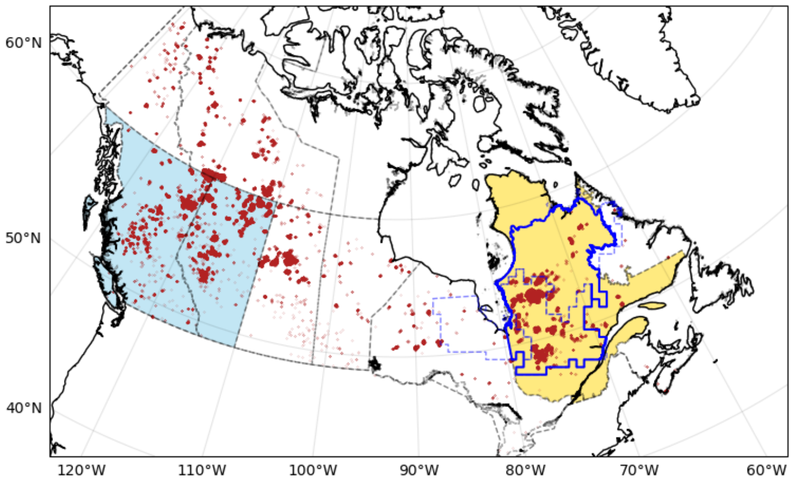

Figure 1: *Red dots mark active fires from January-July 2023 identified with high confidence (>80%) in the MCD14DL MODIS Active Fire and Thermal Anomalies product. The heavily impacted provinces of Alberta and British Columbia in the west, and Québec in the east, are shaded in blue and yellow respectively. The blue outline indicates the study region; blue dashed lines indicate the boundaries of the three homogeneous fire regions included in the region (clockwise from top: Eastern Subarctic, Eastern James Bay, Western James Bay).*

1.1 Event definition

In this study we focus on the fires in eastern Canada, which experienced a particularly severe fire season in 2023, as discussed above. The study region, outlined in blue in Figure 1, is obtained by merging two of the homogenous fire regions (HFRs) proposed by Boulanger et al (2014): these are the Eastern James Bay and Eastern Subarctic regions, and that part of the Western James Bay region that falls within the province of Québec. This selection ensures that the study region falls into one time zone, and so avoids introducing discontinuities into the computed fire weather index. By considering aggregated HFRs, rather than an entire province, we aim to ensure that we consider a region that is relatively homogeneous in terms of its climatology and its vegetation cover, while still covering the worst-affected areas.

Wildfires are complex phenomena that are not driven solely by climate, but also by vegetation properties, land-cover and human activity. Quantifying the effect of climate alone on realised wildfires - for example, on the observed burned area or number of fires - is very difficult (Lui et al., 2022). In addition, fire data are known to be incomplete before 1972 in the study area (NRCan, 2023) As such, we only comment on trends in fire-weather conditions, not on wildfire activity. The indices considered are derived from the daily fire weather index (FWI), details of which are given in Section 2.1.

To reflect the extent and duration of the extreme fire weather across the region, we will use the cumulative daily severity rating (cumDSR). The DSR is a scaled power transformation of the FWI[1], and reflects how difficult a fire is to suppress once ignition has occurred; it is commonly used for assessing fire weather on monthly or longer timescales (Van Wagner, C. E. 1987). Because the 2023 fire season is not yet finished at the time of writing, we consider the cumulative DSR from January to July each year, averaged over the region, as a measure of the total intensity over the region during the first months of the fire season. Days outside of the fire season contribute zero to the cumulative DSR; in years where the fire season has no detectable 'end', the season is assumed to finish on December 31st, and the next to begin on January 1st.

To capture the intensity of the fire weather season, we take the annual maximum of the 7-day moving average of the FWI at each grid cell, then take the mean of these values over all cells in the study region. This index is denoted FWI7x. This index has been used in previous attribution studies (eg. van Oldenborgh et al. (2021)), where it has been found to have a good correlation with the area burned. Note that, because we take the annual maximum of the FWI before the spatial mean, this index does not correspond to the fire weather over a particular period: rather, it reflects the maximum intensity for the whole season. For that reason, for each year we take the annual maximum over all available months, even though the 2023 fire weather season is still ongoing at the time of writing: annual maxima of the 7-day FWI typically occur in June or July, so the maximum of the 2023 season to date may be taken as comparable to the seasonal maximum in any other year, although there is of course a possibility that it may be exceeded during the latter part of the fire season.

2 Data and methods

2.1 Calculation of the Fire Weather Index

The FWI consists of three initial subindices that are calculated using temperature, relative humidity and wind speed at 10m recorded at noon, as well as 24-h precipitation. These subindices are the fine fuel moisture code (FFMC), the duff moisture code (DMC), and the drought code (DC), with values from the previous day feeding back into the system to model long-term changes in fuel moisture. As shown in Figure 2, these three subindices are combined via the initial spread index (ISI) and the buildup index (BUI) to generate the final FWI value.

[1] $DSR = 0.0272 FWI^{1.71}$

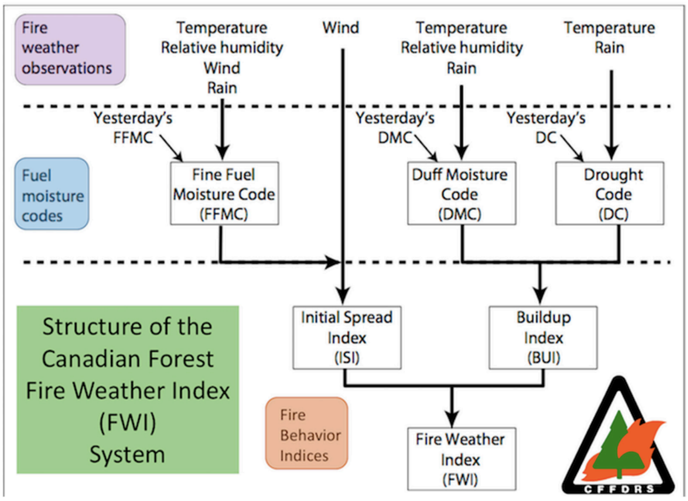

Figure 2: *Structure of the Canadian Forest Fire Weather Index (Van Wagner, C.E (1974); image courtesy of UQAM)*

The system for calculating the FWI was taken from Wang et al. (2015), with an adaptation made for the effect of overwintering on the DC. The fire weather index is applicable throughout the fire season, with the initial sub-index values being set to default initial values after snow-melt; however the long timescale response of the DC means that both cumulative winter precipitation and the DC at the end of the previous season can have an effect on the DC at the start of the next season. Following McElhinny et al. (2020), the fire season is deemed to start after three consecutive days of no snow cover following winter snow cover; or, where no winter snow cover occurred, after three consecutive days with a temperature higher than 12C. The season endpoint follows three consecutive days with a temperature lower than 5C. If the overwinter precipitation was greater than 200mm, it was assumed that moisture was sufficiently replenished for the default DC start value (reflecting non-drought conditions) to be taken. The overwintering formula was taken from Hanes et al. (2020), calibrated following advice from the Canadian Forest Service[2]. A summary of the version of the FWI used can be found on the UQAM website.

The FWI was calculated from hourly reanalysis data, and three-hourly climate ensemble data. The index was calculated using the noon temperature, relative humidity, surface windspeed, snow-depth and antecedent precipitation in the prior 24 hours. When noon values were not given in climate ensembles, the closest available time was taken.

2.2 Observational data

The active fire information shown in Figure 1 is taken from NASA's Fire Information for Resource Management System (FIRMS) moderate resolution imaging spectroradiometer (MODIS MCD14DL) Collection 6. MODIS uses a contextual algorithm (Giglio et al., 2003; Giglio et al., 2016) to detect active fires. Each pixel is classified according to the type of fire detected, along with an associated confidence level, based on the presence or absence of the mid-infrared radiation information typically emitted from fires. Pixels are 1km^2, therefore this is approximately the minimum size of the fires detectable by MODIS. To minimise the risk of false positive detections, only fire pixels assigned a confidence above 80% are retained.

[2] The calibrated coefficients used in equations 1 and 2 of Hanes et al. (2020) were a = 1 and b = 0.75.

Because of the large number of high-resolution weather variables required to calculate the FWI, we are restricted to using a single dataset in the observational analysis: the ERA5 reanalysis product (Hersbach et al., 2020) produced by the European Centre for Medium-Range Weather Forecasts. This product covers the globe at 0.25° resolution, starting in 1940. The variables from ERA5 are not directly assimilated, but are generated by atmospheric components of the Integrated Forecast System (IFS) modelling system. Previous studies have found the FWI to be sensitive to the choice of reanalysis product used (Krikken et al., 2019); however, ERA5 is the product used operationally to monitor fire risks by ESCER, so we have confidence in the reliability of the results.

As a proxy for anthropogenic climate change we use the (low-pass filtered) global mean surface temperature (GMST) taken from the National Aeronautics and Space Administration (NASA) Goddard Institute for Space Science (GISS) surface temperature analysis (GISTEMP, Hansen et al., 2010 and Lenssen et al., 2019).

2.3 Climate model and experiment descriptions

The range of models available for use in fire weather attribution is limited by the requirement to provide local noon temperature, relative humidity (or specific humidity and surface pressure, from which relative humidity can be derived), wind speed and 24-hour accumulated precipitation, along with daily snow values used to estimate the start and end of the fire season. In this analysis, the FWI was computed from three-hourly model output, so noon data was not available: we therefore use the 18:00UTC data, which represents the three-hour period from 11AM-2PM during summer, and from 10AM-1PM during winter (where time steps are labelled at the midpoint, 16:30UTC is used). In some cases, daily mean wind speed was used due to unavailability of 3-hourly data; this is noted below. No bias correction was carried out before computing the FWI.

We use five ensembles of models from climate modelling experiments using different framings (Philip et al., 2020): regional climate models, sea surface temperature (SST) driven global circulation high resolution models, and coupled global circulation models.

CORDEX NAM-22: COordinated Regional Climate Downscaling EXperiment - North American Domain with 0.22° resolution (Ciarlo et al., 2021). These simulations are composed of historical simulations up to 2005, and extended to the year 2100 using the RCP8.5 scenario. The required variables could only be obtained for three runs, all using the same regional climate model to dynamically downscale the output of three independent GCMs.

CRCM5 regional model - The fifth generation of the Canadian Regional Climate Model (CRCM5), developed at the ESCER centre (UQAM, Montreal), is based on a limited-area model (LAM) of the third version of the Canadian Global Environmental Multiscale (GEM) model used for the Numerical Weather Prediction (NWP) at Environment and Climate Change Canada (Coté et al., 1998a and b). The CRCM5 has been widely used under the North America (and Africa) CORDEX protocol, for climate change simulations and various applications (Hernández-Díaz et al., 2019; Poan et al., 2018; Ogden and Gachon, 2019). The CRCM5 simulations use as boundary conditions the Max Planck Institute Earth System Model MPI-ESM-LR (Giorgetta et al., 2013) global climate model, which is a global atmosphere, ocean and land surface coupled model. The simulations cover the historical 1951–2005 and the future 2006-2100 periods, using the RCP8.5 forcing scenario (as used in CMIP5 simulations).

CanESM2-CanRCM4 large regional climate model ensemble (Canadian Earth System Model Large Ensembles - Open Government Portal; Scinocca et al., 2016). The models were produced following the protocols used in the Coordinated Regional Downscaling Experiment (CORDEX), with simulations run to 2005 using CMIP5 historical forcings and then to 2100 using RCP 8.5 forcings following the Coupled Model Intercomparison Project Phase 5 (CMIP5) protocols, which were employed for the CanESM2 large ensemble. The ensemble has 35 members, produced by using CanRCM4 to produce seven independent realisations of each of five realisations of the CanESM2 GCM. The ensemble mean GSAT is used as the explanatory variable during statistical modelling.

HighResMIP SST-forced model ensemble (Haarsma et al., 2016), the simulations for which span from 1950 to 2050. The SST and sea ice forcings for the period 1950-2014 are obtained from the 0.25° x 0.25° Hadley Centre Global Sea Ice and Sea Surface Temperature dataset that have undergone area-weighted regridding to match the climate model resolution (see Table B). For the 'future' time period (2015-2050), SST/sea-ice data are derived from RCP8.5 (CMIP5) data, and combined with greenhouse gas forcings from SSP5-8.5 (CMIP6) simulations (see Section 3.3 of Haarsma et al. 2016 for further details). The required variables could only be obtained for runs from EC-EARTH3P and EC-EARTH3P-HR, with each variant providing two realisations, so these runs are treated as a single ensemble in the analysis. Daily wind speeds were used in place of noon data, and the statistical modelling procedure uses the same GIStemp GMST covariate as the observational analysis.

CMIP6 (Eyring et al., 2016). The ensemble used here consists of simulations from five participating models with varying resolutions. For all simulations, the period 1850 to 2015 is based on historical simulations, while the SSP5-8.5 scenario is used for the remainder of the 21st century. Models are treated as independent, and the statistical modelling procedure uses each model's own 4-year smoothed GSAT as the explanatory covariate. Daily wind speeds were used in lieu of noon data.

2.4 Statistical methods

Methods for observational and model analysis and for model evaluation and synthesis are used according to the World Weather Attribution Protocol, described in Philip et al. (2020), with supporting details found in van Oldenborgh et al. (2021), Ciavarella et al. (2021) and here. The key steps, in sections 3-6, are: (i) trend calculation from observations; (ii) model validation; (iii) multi-method multi-model attribution and (iv) synthesis of the attribution statement.

In this analysis we examine time series of annual maxima of the 7-day FWI (FWI7x) and cumulative DSR between January and July (cumDSR), both averaged over the James Bay region outlined in blue in Figure 1.

A nonstationary generalised extreme value distribution (GEV) is used to model FWI7x: the distribution is assumed to scale with GMST, meaning that the standard deviation of the distribution increases at the same rate as its location. Parameters are estimated using maximum likelihood.

The raw cumDSR values are very skewed, so we first take log10 of the observed time series, then fit a nonstationary normal distribution to the transformed data (the bootstrapped parameter estimates are typically more stable when following this procedure than when fitting a lognormal distribution directly). This distribution is assumed to shift with GMST: that is, the mean of the distribution changes, but the variance remains constant.

For each time series we calculate the return periods, probability ratio (PR; the factor-change in the event's probability) and change in intensity of the event under study for the 2023 GMST and for 1.2C cooler GMST: this allows us to compare the climate of now and of the preindustrial past (1850-1900, based on the Global Warming Index).

3 Observational analysis

3.1 cumDSR: cumulative daily severity rating up to July 31st

Figure 3a shows the cumulative DSR in each grid cell during January-July 2023, the period for which ERA5 reanalysis was available at the time of writing: the most extreme values occur in western Québec, in the areas in which active fires have been detected with high confidence (Figure 1). Figure 3b shows the mean DSR over the study region accumulating over the course of each year, with 2023 highlighted in orange: from late May to early July, the 2023 cumDSR leaps from a fairly low value in to the highest cumDSR recorded in any year in ERA5, highlighting the intensity of the fire weather in the region during June 2023.

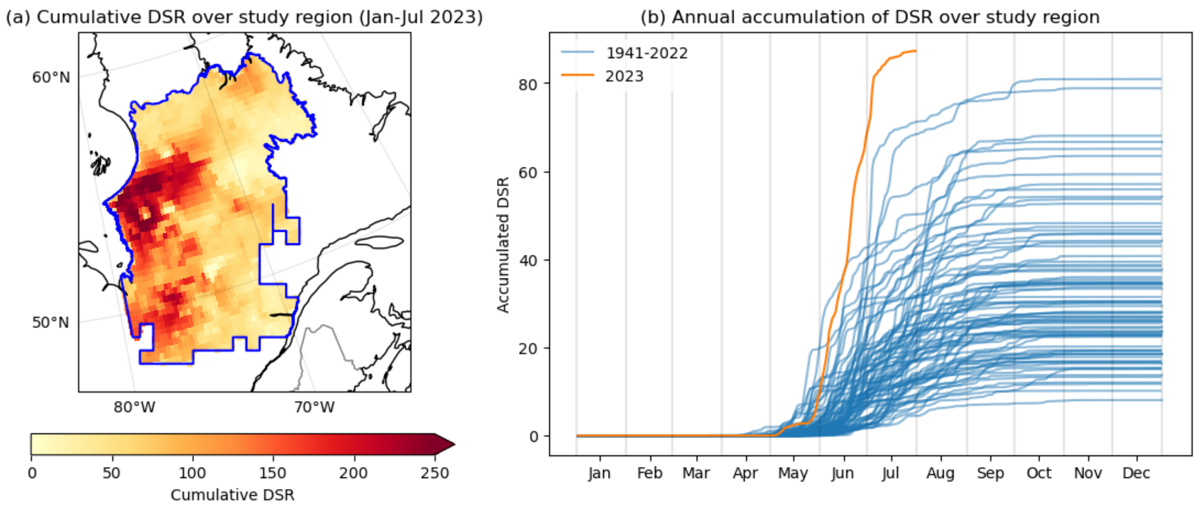

Figure 3: *(a) Map of cumDSR from January-July 2023 within the study region; (b) annual accumulation of daily severity rating (DSR) averaged over the study region, with 2023 values in orange. All data taken from ERA5.*

Figure 4 shows the annual time series of January-July cumulative DSR across the study region, with the 2023 event highlighted in pink. There is a clear upward trend in the time series; the GMST-dependent trend from the statistical model runs approximately parallel to the observed trend in the 15-year running mean from 1970 onwards, although the observed trend is somewhat stronger in the early part of the time series.

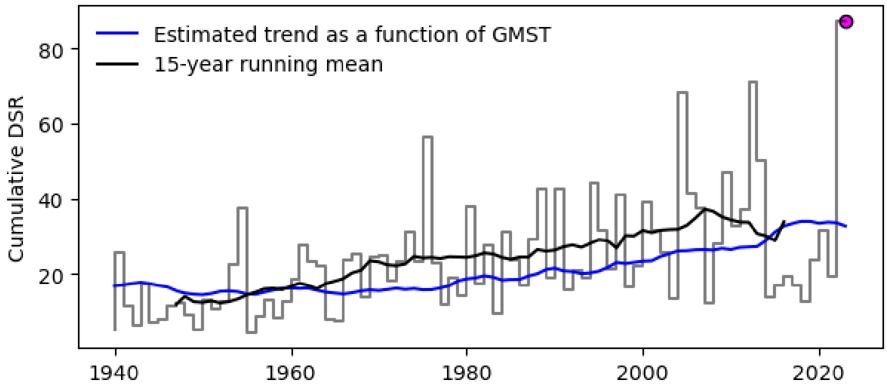

Figure 4: *Time series of annual cumDSR averaged over the study region. The pink dot marks the 2023 event; the heavy black line indicates the 15-year running mean, and the blue line indicates the location of the nonstationary GEV distribution fitted to the data.*

The fitted trend in log10(cumDSR) is shown in Figure 5a, with return level plots in Figure 5b. The log10-normal model fits the data well for high values of log10(cumDSR), although effective return levels are slightly underestimated at return periods of 2-5 years: this is probably due to the unusually low values observed in the last few years. Under this model, the return period of the 2023 cumDSR is estimated to be 25 years in the 2023 climate (95% confidence interval: 10-126). The probability ratio is estimated to be 170 (95% confidence interval: 16 to 3840), indicating that the probability that cumDSR will exceed the observed value of 87.3 in any given year is now much higher than in a preindustrial climate, and at least sixteen times as likely. Under a 1.2C increase in GMST, the cumulative DSR associated with a 25-year event is estimated to have increased by 164%, a statistically significant change at the 5% level (95% confidence interval: 64 - 315%). For the attribution analysis we evaluate the change in intensity and likelihood of a 1-in-25-year cumDSR.

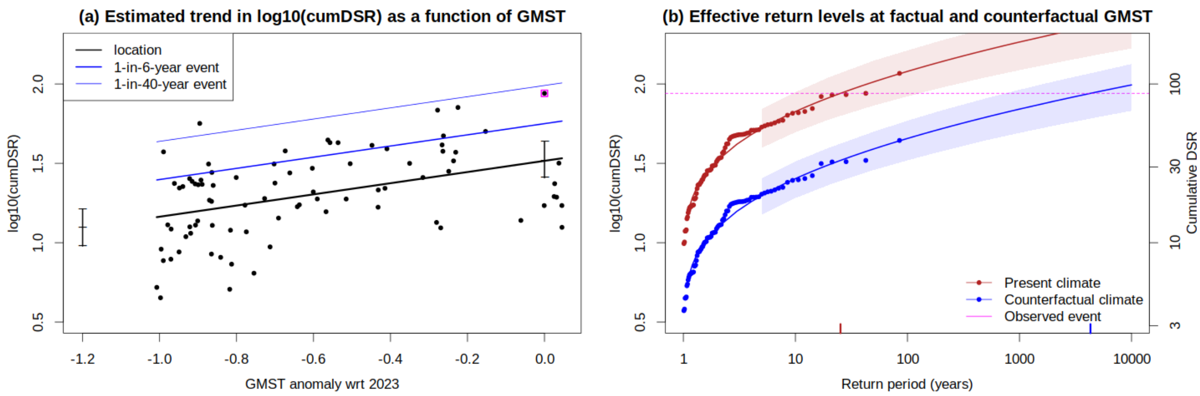

Figure 5*: (a) Linear trend in log10(cumDSR) as a function of GMST. The thick black line denotes the location parameter of the fitted distribution, and the blue lines show estimated 6- and 40-year return levels. The vertical lines show the 95% confidence interval for the location parameter for the 2023 climate and a hypothetical 1.2ºC cooler climate. The 2023 observation is highlighted in magenta. (b) GEV-based return levels for log10(cumDSR) at 2023 GMST (red lines) and 1.2C lower GMST (blue line). Shaded regions represent 95% confidence intervals obtained via a bootstrapping procedure.*

3.2 FWI7x: annual maximum of 7-day FWI

Figure 6a shows the maximum 7-day FWI in each grid cell during January-July 2023, the period for which ERA5 reanalysis was available at the time of writing. The 7-day FWI exceeded 20 - indicating extreme fire risk - in 40% of the cells in the study area during 2023; 90% of cells had FWI7x greater than 10, indicating high or extreme fire risk at some time during the season (based on the provincial threshold for Québec defined by CWFIS). Averaged across the whole study region, 2023 to date has a higher value of FWI7x than any other year (Figure 6b). As in Figure 4, the upward trend estimated by the statistical model is approximately parallel to the observed trend in the 15-year running mean after 1970.

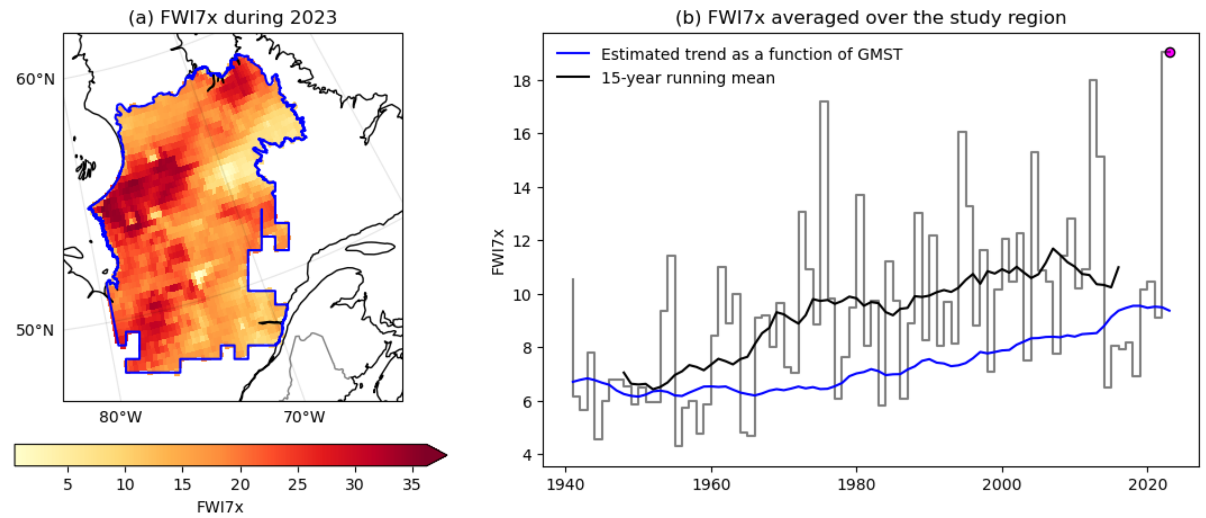

Figure 6: *(a) Map of ERA5 FWI7x within the study region during January-July 2023; (b) time series of FWI7x averaged over the study region. The pink dot marks the 2023 event; the heavy black line indicates the 15-year running mean, and the blue line indicates the location of the nonstationary GEV distribution fitted to the data.*

Figure 7 shows the results of the trend fitting methods described in Philip et al. (2020) applied to the FWI7x time series. The GMST-dependent linear trend is shown in panel a, while panel b shows return level plots. Inspection of Figure 7b suggests that the chosen scaled GEV model fits the data fairly well. In this statistical model, the return period of the 2023 FWI7x is estimated to be 21 years in the 2023 climate (95% confidence interval: 8 - 121). The probability ratio is estimated to be 34 (95% confidence interval: 4.7 to infinite), indicating that the probability that FWI7x will exceed the observed value of 19.03 in any given year is now much higher than in a preindustrial climate, and at least four times as likely. The intensity of FWI7x is estimated to have increased by 64%, a statistically significant change at the 5% level (95% confidence interval: 28 - 123%). For the attribution analysis we evaluate the change in intensity and likelihood of a 1-in-20-year FWI7x value.

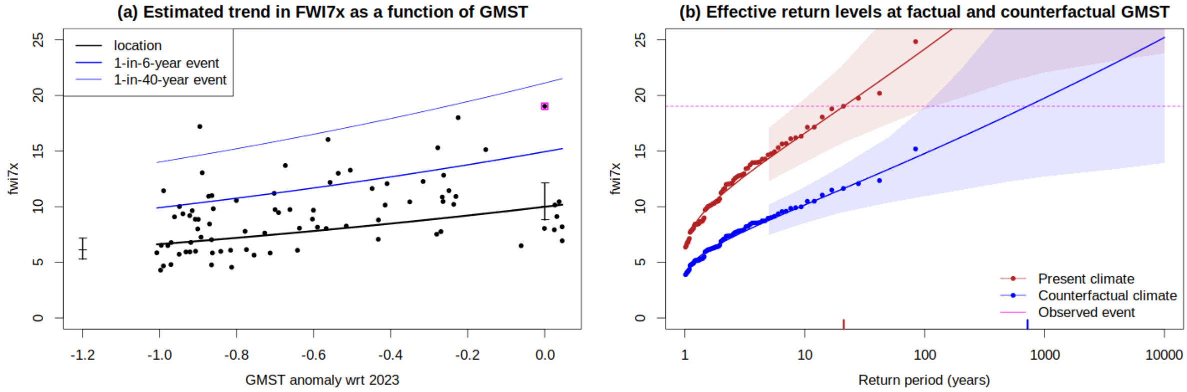

Figure 7: *(a) Linear trend in ERA5 FWI7x as a function of GMST. The thick black line denotes the location parameter of the fitted distribution, and the blue lines show estimated 6- and 40-year return levels. The vertical lines show the 95% confidence interval for the location parameter for the 2023 climate and a hypothetical 1.2ºC cooler climate. The 2023 observation is highlighted in magenta. (b) GEV-based return levels for FWI7x at 2023 GMST (red lines) and 1.2C lower GMST (blue line). Shaded regions represent 95% confidence intervals obtained via a bootstrapping procedure.*

3.3 Trends in subindices

In order to understand the likely factors driving the observed increase in fire weather discussed in sections 3.1 and 3.2, we now briefly consider trends in the subindices and weather variables that contribute to the fire weather index, although no formal attribution is carried out.

Figure 8 shows the annual distribution of the FWI and sub-indices in ERA5 averaged over the study region, with historical years shown in orange and 2023 in black. The red line indicates the 95th percentile of the daily distribution of each index from 1941-2022, smoothed using a 7-day moving window the ERA5; the month of June, during which the most severe fire weather occurred in the region, is highlighted in yellow. From panel (a) we see that the FWI exceeded the 95th percentile of observed values for much of June, particularly at the beginning and end of the month; the initial spread index (ISI, panel b), which is designed to capture the expected rate of fire spread once ignition has occurred, has a similar shape, but slightly less extreme values. The ISI depends primarily on the wind speed and the fine fuel moisture code (FFMC, panel c), which indicates the expected flammability of fine fuel and typically reflects dry conditions on the scale of a few days; the FFMC was relatively high throughout much of May and June, while the daily wind speeds (Figure 9d) were not particularly high for most of the month. The build up index (panel d), which incorporates subindices reflecting drought conditions from weekly to monthly time scales, remained above the 95th percentile for the whole month and the early part of June, exceeding the pre-2023 maximum twice towards the end of the month. This appears to have initially been driven by a peak in the Duff moisture code (DMC, panel e), which remained above the 95th percentile throughout June, and compounded in the later part of the month by an unseasonably early peak in the drought code (panel f), which reached levels that would usually be considered high in mid-August.

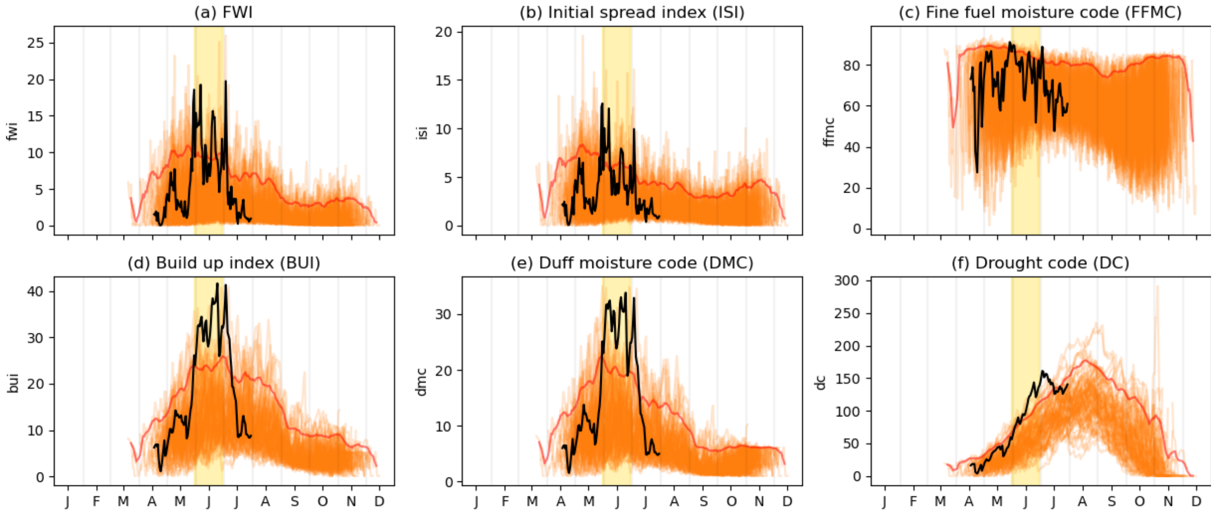

Figure 8: *Distribution of FWI and sub-indices averaged over the study region in ERA5 dataset. Orange lines indicate daily values from 1941-2022; black line indicates 2023 values. Red line shows the 95th percentile of the 1941-2022 distribution on each calendar day, smoothed using a 7-day moving window. June is highlighted in yellow.*

Figure 9 shows annual time series of the May-June mean of key weather variables used in the computation of the FWI, averaged over the study region: this period was chosen to capture the most severe part of the 2023 fire weather season, plus several weeks of antecedent conditions. No trend in May-June precipitation is apparent in this region, but the 2023 value was the third lowest recorded since 1940 in ERA5. At the same time, the mean temperature was relatively high compared to historic values - although not particularly unusual for the recent climate - while the relative humidity was extremely low. In both of these indices a strong trend is evident, with mean relative humidity decreasing as temperatures increase: although no formal attribution is carried out here, past studies (for example, Philip et al., 2022) have linked strong increases in mean temperatures with increasing GMST, so we can be confident that these trends are related to anthropogenic climate change. As noted above, mean wind speeds were relatively low at this time, so it is likely that the increased FWI in 2023 has been caused partly by the unusually dry conditions - both in terms of precipitation and humidity - but partly by increased temperatures driven by anthropogenic climate change.

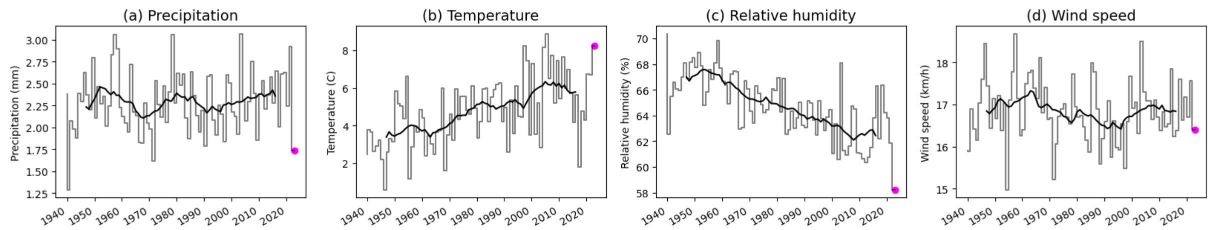

Figure 9: *Time series of April-June mean of key weather variables in ERA5, averaged over the study region: (a) daily precipitation, (b) noon temperature, (c) noon relative humidity, (d) noon 10m wind speed. In each panel the pink dot marks the 2023 event, and the heavy black line indicates the 15-year running mean.*

4 Model evaluation

Climate models are evaluated against the ERA5 reanalysis for their ability to capture the observed distribution of FWI7x and cumDSR, and discarded if the ranges of the key parameters of the fitted non-stationary distribution do not overlap with those estimated from ERA5. The models are labelled as ‘good’, ‘reasonable’, or ‘bad’ for each parameter (dispersion and shape where a GEV is used, and scale where a normal distribution is used). Models are also evaluated in terms of how well they represent the spatial and seasonal patterns of precipitation and temperature over the region. If the model is ‘good’ for all criteria, we give it an overall rating of ‘good’. We rate the model as ‘reasonable’ or ‘bad’, if it is rated ‘reasonable’ or ‘bad’, respectively, for at least one criterion. In the tables below we show the results of the model validation for the three study regions. In each case, if more than five models achieve a ‘good’ evaluation overall, then only these models are included in the attribution; if five models or fewer achieve this, then models deemed ‘reasonable’ are also included. Tables 1 and 2 shows the model evaluation results for FWI7x and cumDSR respectively. All models were found to adequately represent the seasonal cycle and spatial pattern of both temperature and precipitation, so these columns are omitted.

Table 1: *Evaluation results of the climate models considered for attribution analysis of cumDSR. For each model, the best estimate of the scale parameters is shown, along with a 95% confidence interval for each, obtained via bootstrapping. The qualitative evaluation is shown in the right-hand column.*

Data source (observations/models)	**Scale parameter**	**Conclusion**
ERA5	0.242 (0.210 ... 0.268)	
HadGEM2-ES_REMO2015 rcp85 (1)	0.342 (0.272 ... 0.394)	reasonable
MPI-ESM-LR_REMO2015 rcp85 (1)	0.388 (0.315 ... 0.432)	bad
NorESM1-M_REMO2015 rcp85 (1)	0.300 (0.245 ... 0.346)	reasonable
MPI-ESM-LR_CRCM5 rcp85 (1)	0.315 (0.271 ... 0.349)	bad
CanESM2-CanRCM4 rcp85 (35)	0.191 (0.186 ... 0.198)	reasonable
HighresMIP EC-Earth ensemble ssp585 (4)	0.245 (0.223 ... 0.264)	good
EC-Earth3_r1i1p1f1 ssp585 (1)	0.369 (0.312 ... 0.417)	bad
HadGEM3-GC31-LL_r1i1p1f3 ssp585 (1)	0.337 (0.280 ... 0.382)	bad
HadGEM3-GC31-MM_r1i1p1f3 ssp585 (1)	0.302 (0.250 ... 0.348)	reasonable
MIROC6_r1i1p1f1 ssp585 (1)	0.246 (0.209 ... 0.272)	good
MPI-ESM1-2-LR_r1i1p1f1 ssp585 (1)	0.322 (0.274 ... 0.364)	reasonable

Table 2: *Evaluation results of the climate models considered for attribution analysis of FWI7x. For each model, the best estimate of the dispersion and shape parameters is shown, along with a 95%*

confidence interval for each, obtained via bootstrapping. The qualitative evaluation is shown in the right-hand column.

Data source (observations/models)	Dispersion	Shape parameter	Conclusion
ERA5	0.281 (0.240 ... 0.313)	0.040 (-0.17 ... 0.22)	
HadGEM2-ES_REMO2015 rcp85 (1)	0.466 (0.379 ... 0.541)	0.066 (-0.31 ... 0.35)	bad (dispersion)
MPI-ESM-LR_REMO2015 rcp85 (1)	0.523 (0.397 ... 0.590)	-0.047 (-0.38 ... 0.48)	bad (dispersion)
NorESM1-M_REMO2015 rcp85 (1)	0.357 (0.254 ... 0.418)	0.20 (-0.070 ... 0.60)	reasonable
MPI-ESM-LR_CRCM5 rcp85 (1)	0.395 (0.328 ... 0.448)	0.15 (-0.30 ... 0.38)	bad
CanESM2-CanRCM4 rcp85 (35)	0.208 (0.203 ... 0.214)	-0.003 (-0.031 ... 0.021)	bad (dispersion)*
HighresMIP EC-Earth ensemble ssp585 (4)	0.320 (0.292 ... 0.344)	0.071 (-0.0020 ... 0.15)	reasonable
EC-Earth3_r1i1p1f1 ssp585 (1)	0.452 (0.388 ... 0.518)	0.21 (0.057 ... 0.48)	bad (dispersion)
HadGEM3-GC31-LL_r1i1p1f3 ssp585 (1)	0.425 (0.340 ... 0.496)	0.092 (-0.036 ... 0.41)	bad
HadGEM3-GC31-MM_r1i1p1f3 ssp585 (1)	0.392 (0.312 ... 0.475)	0.0030 (-0.23 ... 0.26)	reasonable
MIROC6_r1i1p1f1 ssp585 (1)	0.288 (0.239 ... 0.337)	-0.043 (-0.30 ... 0.12)	good
MPI-ESM1-2-LR_r1i1p1f1 ssp585 (1)	0.432 (0.363 ... 0.490)	-0.021 (-0.18 ... 0.11)	bad

* The CanESM2-CanRCM4 large ensemble failed evaluation due to underdispersion in the distribution of FWI7x. However, due to the size of the ensemble, the confidence interval for the parameter is extremely narrow, making the criterion extremely strict. Given that the shape parameter is well estimated, and that the distribution was found to fit the data well, we decided to reclassify this model as 'reasonable' and so to include it in the analysis.

5 Multi-method multi-model attribution

Tables 3 and 4 show probability ratios (PR) and changes in intensity (ΔI) for ERA5 and for those models that passed evaluation for each index.

Table 3: *Probability ratio and change in intensity for 25-year cumDSR for ERA5 and each model that passed evaluation: (a) from preindustrial climate to the present and (b) from the present to 2C above preindustrial.*

	(a) -1.2C vs present		(b) Present vs +0.8C	
Data source (observations/models)	**Probability ratio**	**Change in intensity**	**Probability ratio**	**Change in intensity**
ERA5	170 (16 ... 3840)	165 (64 ... 316)		
HadGEM2-ES_REMO2015 rcp85 (1)	0.52 (0.13 ... 1.8)	-23 (-50 ... 27)	0.92 (0.52 ... 1.4)	-3.7 (-25 ... 13)

NorESM1-M_REMO2015 rcp85 (1)	2.38 (0.22 ... 26)	29 (-37 ... 152)	2.2 (1.2 ... 3.6)	26 (7.0 ... 42)
CanESM2-CanRCM4 rcp85 (35)	3.3 (2.6 ... 3.9)	25 (20 ... 29)	2.0 (1.9 ... 2.1)	18 (16 ... 19)
HighresMIP EC-Earth3P ensemble ssp585 (4)	2.9 (1.1 ... 9.1)	29 (2.1 ... 66)		
HadGEM3-GC31-MM_r1i1p1f3 ssp585 (1)	49 (16 ... 175)	164 (90 ... 290)	4.9 (3.9 ... 6.9)	39 (34 ... 44)
MIROC6_r1i1p1f1 ssp585 (1)	178 (25 ... 1677)	157 (70 ... 275)	4.4 (2.8 ... 6.7)	30 (20 ... 38)
MPI-ESM1-2-LR_r1i1p1f1 ssp585 (1)	1.2 (0.38 ... 3.2)	6.0 (-26 ... 49)	1.4 (0.99 ... 2.0)	12 (-0.28 ... 23)

Table 4: *Probability ratio and change in intensity for 20-year FWI7x for ERA5 and each model that passed evaluation: (a) from preindustrial climate to the present and (b) from the present to 2C above preindustrial.*

	-1.2C vs present		Present vs +0.8C	
Data source (observations/models)	**Probability ratio**	**% change in intensity**	**Probability ratio**	**% change in intensity**
ERA5	34 (4.7 ... ∞)	64 (28 ... 123)		
NorESM1-M_REMO2015 rcp85 (1)	1.4 (0.032 ... 5.9)	9.5 (-40 ... 54)	1.7 (1.1 ... 3.0)	14 (2.4 ... 24)
CanESM2-CanRCM4 rcp85 (35)	1.9 (1.6 ... 2.2)	8.0 (6.2 ... 10)	1.5 (1.4 ... 1.6)	5.8 (5.2 ... 6.4)
HighresMIP EC-Earth ensemble ssp585 (4)	2.7 (1.3 ... 7.3)	20 (4.5 ... 39)		
HadGEM3-GC31-MM_r1i1p1f3 ssp585 (1)	3.8 (1.4 ... 35)	30 (6.2 ... 29)	2.4 (1.4 ... 4.9)	15 (7.6 ... 22)
MIROC6_r1i1p1f1 ssp585 (1)	2.0 (1.5 ... 11)	9.9 (4.9 ... 23)	1.8 (1.3 ... 2.9)	8.7 (3.8 ... 14)

6 Hazard synthesis

For the two indices defined in Section 1.1 we evaluate the influence of anthropogenic climate change by calculating the probability ratio and change in intensity for both observations and climate models. Models which do not pass the validation tests described in Section 4 are excluded from the analysis. The aim is to synthesise results from models that pass the evaluation along with the observation-based products, to give an overarching attribution statement. Figure 10 shows the changes in probability and relative intensity of a 1-in-25-year cumulative DSR event for the observations (blue) and models (red). The best estimate for each dataset is marked with a black triangle. A term to account for intermodel spread is added in quadrature to the natural variability of the models: this is shown in the figures as white boxes around the light red bars. The dark red bar shows the model average, consisting of a weighted mean using the (uncorrelated) uncertainties due to natural variability plus the term representing intermodel spread (the inverse square of the white bars). Observation-based products and models are combined into a single result in two ways. Firstly, we neglect common model uncertainties beyond the intermodel spread that is depicted by the model average, and compute the weighted average of models (dark red bar) and observations (dark blue bar): this is indicated by the magenta bar. To account for the fact that, due to common model uncertainties, model uncertainty can be larger than the intermodel spread, we also show an unweighted direct average of observations (dark blue bar) and models (dark red bar) contributing 50% each, indicated by the white box in the synthesis figures.

As discussed in Section 3.1, ERA5 has a relatively strong increase in both probability ratio (best estimate 170; 95% confidence interval 16.4 - 3840) and intensity (best estimate 39.1; 23.4-50.2%) of cumDSR; there is less agreement between the models, perhaps reflecting additional variability due to fluctuations in the timing of the start of the fire season, but overall they still indicate a likely increase in the probability and intensity of 25-year cumDSR events (dark red bar). The weighted synthesis of models and observations (magenta bar) gives a best estimate of 53.4 for the probability ratio (7.03 - 621) and of 128% for the change in intensity (50.6 to 238%). Given the wide range of uncertainty in both the observations and models, we take the lower bound of the weighted synthesis (magenta bar) as a conservative estimate, giving a probability ratio of 7.03 and a change in intensity of 50.6%. There is slightly stronger consensus between the models about the likely changes in probability and intensity after a further increase of 0.8C (that is, with total warming of 2C with respect to the preindustrial climate), although the projected changes are not statistically significant: the probability ratio is estimated to be 2.23 (0.633 - 7.85), with a further increase in intensity of 21.2% (-4.14% to +52.9%).

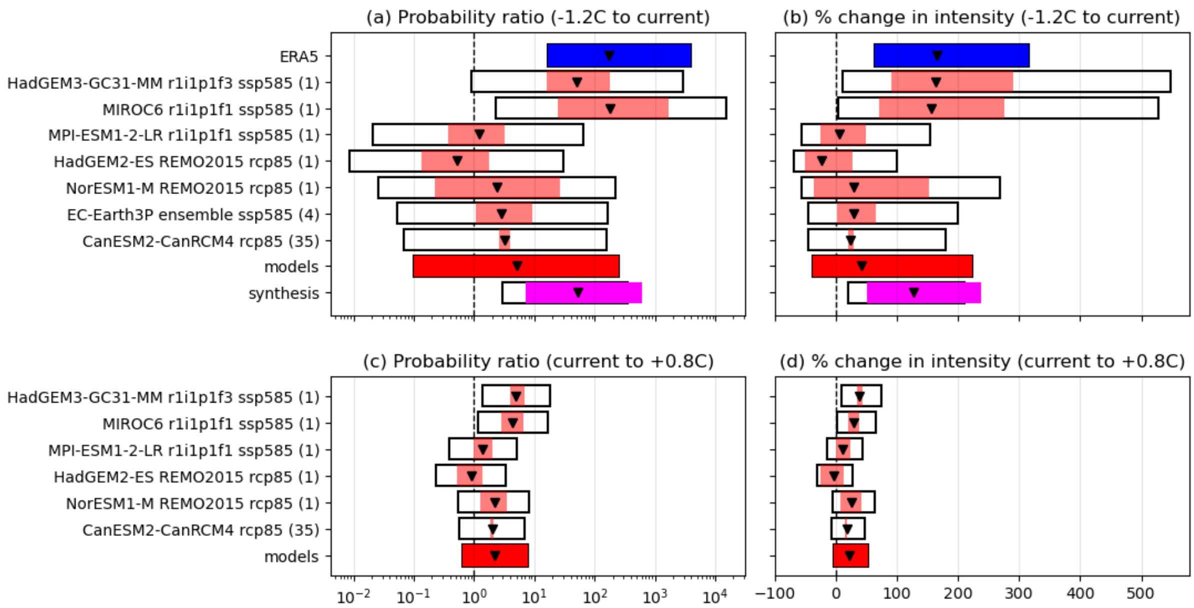

Figure 10: *Synthesis of (left) probability ratios and (right) relative intensity changes when comparing the return period and magnitudes of Jan-July cumDSR in the study region: (top) between the current climate and a 1.2C cooler climate and (bottom) between the current climate and a 0.8C warmer climate (ie. with total warming of 2C). Numbers in brackets show the number of members in each ensemble. See text for further details.*

Figure 11 shows the same synthesis plots for FWI7x. Again, ERA5 has a relatively strong increase, although the uncertainty around these estimates is very large: the upper limit of the change in probability of a 20-year event is infinite, and is truncated here to 1000. The models show a somewhat weaker trend, although all but one indicate a statistically significant increase in both likelihood and intensity of this kind of event. Agreement between the probability ratios estimated by the models is strong enough that no additional term is required to capture inter-model spread, indicated by the absence of white bars around the models in Figure 11a.

Due to the large difference between the trend in ERAs and the models, the unweighted synthesis (indicated by the white boxes in the bottom row of Figures 10a and b) is somewhat higher than the weighted synthesis indicated by the magenta box: given the extremely large uncertainty on the ERA5 best estimate, and the fact that only one observational dataset is used in this study, we therefore take the more conservative estimate given by the weighted synthesis. The probability ratio is estimated to be 1.9 (95% confidence interval: 1.66 - 2.24) and the relative change in intensity 17% (7.8 - 26.6%). Between the current climate and a further increase of 0.8C, the probability ratio is estimated to be 1.57 (1.31 - 1.88), with a further 9.3% increase in intensity (2.6-16.4%).

Combining lines of evidence from the synthesis results of the past climate, results from historical and future projections and physical knowledge, we conclude that January-July cumulative DSR like that experienced in 2023 is at least seven times more likely to occur, and was 50% higher than it would have been without climate change; that peak fire weather intensity (FWI7x) like the 2023 event is at least twice as likely to occur, and around 20% more intense, than it would have been without human-induced climate change; and that this trend is projected to continue if warming continues.

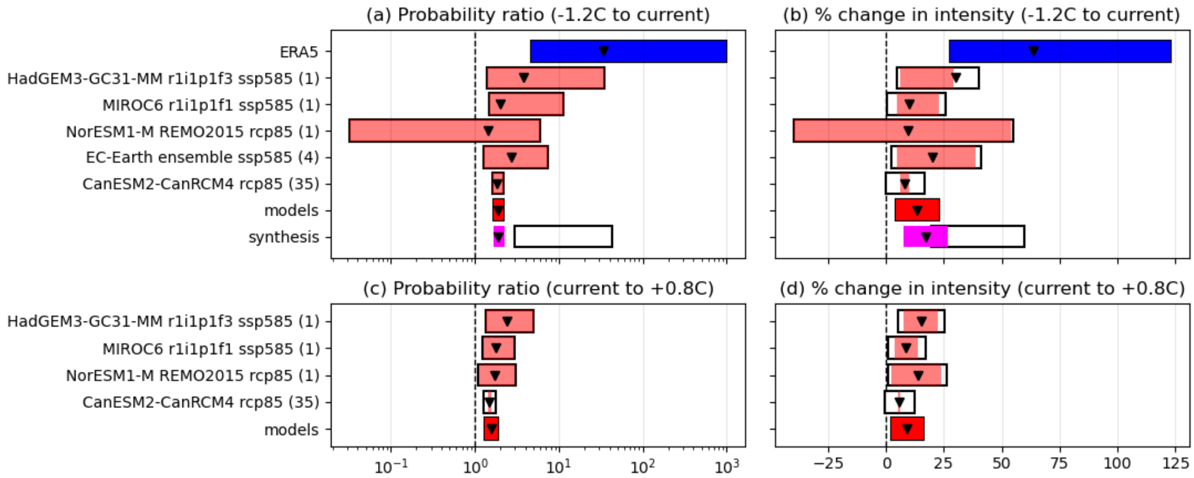

Figure 11: *Synthesis of (left) probability ratios and (right) relative intensity changes when comparing the return period and magnitudes of FWI7x in the study region: (top) between the current climate and a 1.2C cooler climate and (bottom) between the current climate and a 0.8C warmer climate (ie. with total warming of 2C). Infinite probability ratios are truncated at 1000. Numbers in brackets show the number of members in each ensemble. See text for further details.*

7 Vulnerability and exposure

The IPCC characterises risk as a product of hazard, exposure, vulnerability and coping capacity (IPCC, AR6). In extreme event attribution studies, analysing the vulnerability and exposure context of the event draws a critical link between the hazard and the impacts that are felt, and helps highlight ways in which these impacts may have been reduced or exacerbated.

In the following section, we examine key themes of vulnerability and exposure in relation to the wildfires. Given the widespread nature of the 2023 wildfires beyond the event definition for this study, we refer to the whole of Canada in some instances, with specific references to systems and realities in the study area of Québec in others.

7.1 Wildfire legislation and funding

Canada has a complex and bolstered legal framework regarding wildfire prevention, management and response (Tymstra et al., 2020), with shared responsibilities at the federal, provincial/territorial, and local levels, including Indigenous self-governed land.

Civil protection and disaster laws apply to wildfires in inhabited areas but wildfires that do not not affect people or goods are exclusively a provincial responsibility as it relates to their forest management competency. Therefore, every province and territory has developed bespoke legislation to prevent, detect and manage wildfires, resulting in different measures and permits being in place in each region (Gouvernement du Québec, 2023b). If provincial and territorial firefighting capacity is insufficient, the law enables these governments to ask for federal support, regulated by the Emergency Management Act (EMA). The Act includes an article about potential joint emergency management plans with the US (S.C., 2007). Canada has also signed long-term cooperation agreements with Australia, Costa Rica, Mexico, New Zealand, South Africa, and Portugal. These international agreements of mutual comprehension play a crucial role in the battle against wildfires. They represent tactical and low-risk components that secure firefighting capacity during critical periods, facilitating collaborative efforts across the spectrum of forest fire suppression activities.

Municipalities hold partial responsibility for the protection of people and goods against all wildfires through the design and implementation of municipal emergency plans compliant with other legislation. Municipality or Indigenous self-governed land can request support from their provincial or territorial Government if their capacities are insufficient to manage a wildfire, in case of an evacuation for instance. Additional provincial and territorial legislations are in place related to civil and infrastructure protection and the training of firefighters among other things (Gouvernement du Québec, 2023a).

In recent years, numerous legal cases have reinforced the legal framework of enforcement with conviction of private companies, individuals responsible for wildfires in different provinces and territories. Legislation also often restricts the use of prescribed burning (Kohn, 2018) and other Indigenous Fire Management practices which can be effective wildfire prevention measures (see below). The consequences of wildfires for youth have also been mentioned in ongoing Canadian climate litigation cases (*La Rose v. Her Majesty the Queen*, 2019).

The wildfire funding landscape is complex and involves a variety of civil society actors and government collaborations. Indeed, national roundtables on wildfire prevention and mitigation by the Canadian Council of Forest Ministers (2022) involved over 100 stakeholders with key takeaways including the importance of localised strategies and whole-of-society collaboration to meet the diverse needs on the ground. In Québec, the *Société de protection des forêts contre le feu* (SOPFEU) is a non-profit organisation in charge of protecting forests, detecting and managing wildfires working closely with the Government, forest industry and major private landowners (SOPFEU, 2023b). Most provinces and territories have similar agencies, often part of their Ministry of Forests. In parallel, investments on wildfire prevention are varied. For instance, in 2023, Natural Resources Canada received support through the Government of Canada Adaptation Action Plan for a Wildfire Resilient Futures Initiative to "the FireSmart Canada program; increase Canadians' resilience to wildfire while building wildland fire knowledge through research and pilot projects on fire risk reduction measures; and create a Centre of Excellence for Wildland Fire Innovation and Resilience" (Public Safety Canada, 2023).

7.2 Forest and wildfire management

Forest management is a key driver of wildfire risk reduction. In the case of this event, the type of forest, the economic activity it begets, and various approaches to its management are essential components.

7.2.1. Ecological landscape

Forest type, and the amount of debris and flammable material within it, have an influence on the extent and severity of any wildfire. In this case, the wildfires occurred primarily in the Canadian boreal forest, a landscape where change is driven by disturbances such as wildfires and pest outbreaks, and where a majority of the trees are slow-growing conifers and a diversity of underbrush plants (Brandt et al.. 2013). Wildfire is a natural process in this type of forest, essential for the ecological health and biodiversity of the land, and has shaped its current ecology (Brandt et al.. 2013).

7.2.2. Forestry sector dynamics

A significant proportion of the Canadian boreal forest is used by the forestry sector which plays an important role in the wildfire risk and management of the region, and in the story of this event. Indeed, in 2019, Canada's forest sector added $23.7 billion to the GDP, making it a global leader in forest product trade (NRCan, 2020). In Québec more specifically, this sector holds great importance, contributing $20.6 billion in revenue and $5.1 billion to real GDP in 2020 (NRCan, 2020). In Québec, managed forests span 58.3 Mha with 43.4 Mha considered productive. About 92% of these forests are publicly managed. Québec's forest management adheres to sustainability principles for long-term productivity. As mentioned earlier in this report, wildfires this year in Québec have affected more than 1.5 Mha within the province's commercial forest, potentially greatly impacting its forest sector. Indeed, the industry faces potential threats from climate-induced shifts in wildfires (Williamson et al., 2009; Price et al., 2013; Gauthier et al., 2014, 2015; Boucher et al., 2018).

Previous studies have already warned that climate-induced increases in wildfire activity in Canada in the upcoming decades could pose ecological and societal risks (Duerden, 2004; Hope et al., 2016) notably by bringing substantial long-term financial losses, jeopardising jobs, including in remote regions. Notably, prior assessments (Gauthier et al., 2015; Boulanger et al., 2017; Boucher et al., 2018) have highlighted that increased wildfire activity could make harvesting rates unsustainable in many forest management units, especially in Québec's regions that were affected by this year's fires. These regions which are already experiencing short wildfire intervals and low productivity are increasingly vulnerable to regeneration failures due to changing burn rates or management practices (Splawinski et al., 2019a and b; Cyr et al., 2021). In this context, timber shortages are to be expected if harvesting rates are not revised (McKenney et al. 2022; Daniel et al., 2017; Brecka et al., 2020). In the future, no-regret measures may have to be prioritised (Bernier and Schoene, 2009; Raulier et al., 2015). A status quo strategy could directly affect boreal forest's resilience, with cumulative impacts of wildfires and anthropogenic activities putting the ecosystem out of its natural range of variability (Bergeron et al., 2010).

7.2.3. Forest management approaches

Managing the ecological role of wildfires, their potential human threat, and various interests requires a delicate balance. In unpopulated areas in the region, wildfires are often left to burn to cultivate ‘good fire' (Tavernise, 2023). Logging and industry requirements have been arguments for fire management practices which strongly reduce burnable vegetation through thinning and removing or redistributing fuels (such as grass, dead leaves, shrubs, etc) (Beverly et al., 2020; Blanco et al., 2015; Olson et al., 2023). However, recent research points to an increase of wildfire risk associated with strong wildfire suppression approaches in the region (Parisien et al., 2020). Controlled burning has been long recognized by Indigenous communities in these areas as a critical wildfire management tool (Tymstra et al., 2020. However, legal barriers to controlled burning mirror colonial legacies and challenges to Indigenous knowledge around the world (Copes-Gerbitz et al., 2021; Hoffman et al., 2022; Christianson, 2015), and recent research has supported calls for a fire governance shift closer towards the use of traditional knowledge (Nikolakis and Roberts, 2021). Some have argued that a diverse toolbox of wildfire management techniques, including a combination of controlled burns and brush management is necessary to effectively manage wildfire risk at scale (Tymstra et al., 2020).

7.3. Wildfire ignition prevention

Lightning is often pinpointed as the leading cause of wildfires in Canada (Tymstra et al., 2020), but some studies attribute up to 55% of the wildfires to human activities, including smoking, campfires, and railroads (Hesseln, 2018). Generally as well, areas with higher population density may tend to have a higher incidence of human-caused wildfires. Research links fire prevention education to a reduction in the number of preventable wildfires (see e.g. Prestemon et al., 2010; Pooley et al., 2021). Championing wildfire prevention among homeowners and municipalities since 1999, FireSmart Canada is a national program which provides an educational framework, tools, and recommendations for fire preparedness (FireSmart Canada, n.d.). At household level, families are for instance encouraged to clear vegetation around the house, and communities to mechanically thin bushes and trees (Asfaw et al., 2022). Since 1922, an annual national fire prevention week has moreover been observed, with varying themes contextualised to local risks (see e.g. Government of Québec, 2023; National Fire Protection Association, 2023). Despite these efforts, the Government of Canada (2023) still regards the gaps in public fire risk knowledge as "notable."

7.4 Wildfire response

In the case of the studied wildfires, the emphasis has been on the containment away from human settlement, infrastructure, and assets. This is likely partially due to the sheer extent of the wildfires and a documented funding gap between preparedness requirements and growing need which has forced agencies to constrain their protection areas to the high-priority at risk locations (Tymstra et al., 2020). Additional document challenges to wildfire response also include personnel and technical capacity, as well as competing priorities with limited financial resources at the municipality level, which limit FireSmart principles and/or local initiatives (Tymstra et al., 2020).

Most communities directly exposed to the wildfires were among the most remote in the country. Fly-in communities which are usually accessed by air transport for most of the year are highly threatened by wildfires (Transport Canada, 2021) yet risks to safely fly and land planes significantly impact response capacity (Snowdown, 2023). In early July, it was also calculated more than 75% of people in Canada under evacuation orders belonged to Indigenous communities (AP, 2023). This is in line with previous findings which indicate that Indigenous peoples in Canada face a 30% higher probability of being displaced by and experiencing the adverse impacts of wildfires (Hoffman et al., 2022).

7.4.1 Detection and warning

The Department of Natural Resources (NRCan), a federal-level department, supports the detection and monitoring of wildfires, providing updates to the Canadian Interagency Forest Fire Centre (CIFFC) and in support of the public safety mandate (Tymstra et al., 2020). The information collected by NRCan is shared on an online platform, the Canadian Wildland Fire Information System (CWFIS) which maps out fires and labels them according to the Canadian Forest Fire Danger Rating System (CFFDRS) (Tymstra et al., 2020). The rating provided under CFFDRS is calculated using a number of variables including weather, fire behaviour (ex. wildfire intensity and rate of expansion), and seasonal forecasts (Tymstra et al., 2020). Fire agencies and relevant actors rely on this data to inform the resources needed to respond to the forecasted conditions (Tymstra et al., 2020).

Updates from the CIFFC are also used for public communications of wildfires (Tymstra et al., 2020). As part of Canada's 'all-hazard' approach towards managing both manmade and natural disasters, the procedure for communicating public information about wildfires, and subsequently, air pollution are standardised through the following channels (Tymstra et al., 2020):

- AlertReady: the National Public Alerting System which sends information followed by an audio alert to mobile phones, TVs and radios. During this wildfire, information sent through AlertReady to mobile devices in the province of Alberta were delayed due to challenges faced by wireless service providers in disseminating the information (Wong, 2023).
- WeatherCAN provides weather forecasts and alerts for extreme weather-related events (Government of Canada, 2022). As well as radio and television broadcasts, and Twitter (GovCan, n.d.).
- Public Weather Alerts for Canada and Weather Radio are also provided with the wildfire information and dissemination accordingly (Government of Canada, 2022b).

Additionally, provinces, territories, and municipalities issue evacuation alerts and orders for wildfires with the emergency organisations at each level providing information on evacuation routes and actions (Government of Canada, 2023).

7.4.2 Wildfire protection

Record-breaking evacuations were conducted during this season. As of July 6th, the wildfire season was estimated to have displaced up to 155,856 people, the highest in four decades (AP, 2023). Various other response operations took place. For instance, Canadian Red Cross assisted with wildfire response across the country by supporting these evacuations, providing impacted families and individuals with recovery supports such as financial assistance, mental health supports, hygiene kits, temporary housing, and navigating insurance processes (CRC, 2023a; CRC, 2023b; CRC,2023c).

To tackle the immediate disruptions to everyday life, the Canadian government has outlined a series of social protection interventions for those unable to work due to displacement or due to the general hazardous conditions of wildfires such as poor air quality. This includes access to Employment Insurance to offset income loss due to the wildfires (ESDC, 2023), as well as 'Work-Sharing Special Measures' for impacted businesses (ESCD, 2023). Further studies about the effects of these interventions will be important to examine. For this particular series of wildfires in May 2023 to June

2023, a request for Federal Assistance was submitted by the Province of Quebec and was approved on June 3 (GovCan, 2023). The request was to engage Canadian Armed Forces to provide personnel, airlift resources, and infrastructure support for two weeks with potential extension of their services. Additional requests, included by were not limited to logistic support from Public Services and Procurement Canada and Public Health Agency of Canada, personnel from the Royal Canadian Mounted Police and Parks Canada, program assistance from Employment and Social Development Canada and response and recovery assistance by the Indigenous Service Canada's Emergency Management Assistance Program (PSC, 2023).

To protect the health of those impacted by wildfires, Health Canada and the Public Health Agency work with agencies across all levels to decrease the risks of air pollution through initiatives such as providing advice and information about the Air Quality Health Index, technical guidance and provisions of equipment (ex. Air monitoring equipment and N95 respirators) (Health Canada, 2023). Additional mental health supports are available through crisis response lines for children, youth and adults (YMHC, 2023). Comprehensive health supports are integral as studies on previous Canadian wildfires indicate that individuals who have been forcibly displaced by wildfires experience both mental and physical health ailments after the event (Mohamed, 2020). For instance, in the case of the 2016 wilfire in the Regional Municipality of Wood Buffalo, Alberta (a region which includes Fort McMurray), children between the ages of 11-18 demonstrated a higher probability of depression, suicidal ideation and decreased self-esteem in comparison to children of the same age in Red Deer, Alberta, who did not experience the wildfire (Mohamed, 2020).

7.4.3 Containment and extinguishment

As mentioned above, containment strategies for wildfires have aimed to allocate much of the scarce resources to protecting people and communities rather than total extinguishment (Tavernise, 2023). For these wildfires in particular, the sheer size of the multiple, wide-spanning fires and a shortage of wildland firefighters in the country has posed challenges to containment (Williams, 2023). Indeed, as of late June and early June, Canada had already exceeded the record for area burned due to wildfires within a calendar year (Rabson, 2023). To fill the shortage of wildland firefighters and national response capacity, international response relationships mentioned previously was leveraged - in June 2023, approximately 1,207 international fighters were deployed in Canada from across the world including the United States of America, Australia, South Africa, Portugal, France, Spain, Chile, Costa Rica, and New Zealand (Wong, 2023). Alongside these efforts, the SOPFEU adapted their fire training course to produce 350 auxiliary fire combatants through intensive two and a half day courses to boost domestic response capacity (Radio-Canada, 2023).

7.5 Air quality management and protection

The Canadian wildfires have severely impact air quality locally in Canada, and in the neighbouring United States with Air Quality Index (AQI) values frequently exceeding safe levels in the midwest and northeast USA, and in some cases approaching record levels (e.g. on June 7th AQI reached 341 in New York City, considered hazardous for all residents) (CNBC, 2023). Similarly, in southern Ontario, including the cities of Ottawa and Toronto, air quality reached the "very high risk" level forcing officials to cancel public events and reduce hours for outdoor public services (CTV News, 2023). The health impacts of wildfire smoke are well-studied and include an increased risk of all-cause mortality, and respiratory infections, as well as exacerbating existing respiratory issues such as asthma and chronic obstructive pulmonary disease (Reid et. al., 2016). To reduce potential impacts to human health, local authorities, such as New York State, issued air quality alerts via traditional and social media as well as activating emergency notifications on highways and in public transport systems. New York City warned residents to stay indoors and avoid strenuous activity if outdoors. The State also released 'hundreds of thousands' N95 masks to residents. Montanna, Colorado, Iowa, Minnesota and other States initiated similar measures (AP 2023; Vox 2023; NYS 2023). Depending on synoptic weather conditions, the wildfire smoke will continue to be an intermittent issue for Canada and its neighbours while the wildfires burn.

7.6 Recovery and adaptation

As the wildfire season continues, and moving towards recovery phases, communities and governments at various levels will begin to engage in land and ecosystem restoration, infrastructure repairs, insurance payouts, and more. As is often the case after events such as these, a period of after-action reviews and discussion are expected to take place and will be critical regarding preparedness for and adaptation to future events. For instance, in 2029, the Canadian Government is planning to launch its WildFireSat wildfire monitoring system (Government of Canada, n.d.), and other initiatives are likely to be explored as well.

7.7 V&E Conclusion

The drivers of risk related to wildfire are multiple and complex: from forest characteristics to forest management approaches to wildfire legislation and policy, all the way to disaster response at various levels. Wildfires are part of the ecology of the Canadian boreal forest and pose a risk to both the communities that live there and the forestry sector which covers a large proportion of the area. Recent research has argued that a balance of different management techniques, with an emphasis on local Indigenous knowledge and practices is required to adequately manage wildfire risk in these areas. Dedicated adaptive strategies and resources will be essential to mitigate and prevent further impacts on ecosystems, the forestry sector, and local communities in the country in the coming decades (Boulanger et al., 2023). Canada also has an extensive legislative, policy, and financial landscape regarding wildfires. Existing warning, protection, and containment measures were deployed to protect people and communities from the direct impacts of the fires and the indirect impacts on air quality degradation that were seen across Canada and the United States, illustrating the transboundary nature of these types of events. As with all disasters, more vulnerable people and communities are hit the hardest, be it remote communities in which evacuations were particularly difficult to conduct or people with respiratory illnesses being forced inside due to bad air quality.

The challenges posed by this year's wildfires as well as the projected increases in wildfire weather risk raise important adaptation questions, including: How will increasing wildfires risk affect vulnerable and exposed communities and people, and what coping capacity is needed? How should fire management and prevention approaches be adapted to address changing risk? How should cities manage exacerbating air quality risks; what air quality protection measures are feasible and what co-benefits might they have? How should limited resources be distributed across early warning, response, and longer-term adaptation? What are the hard and soft limits in adapting to wildfires in Canada and around the world? And far more. In the coming weeks and months after the wildfires, after-action reviews and adaptation conversations will be critical.

Data availability

Time series used in the analysis are available via the Climate Explorer.

References

All references are given as hyperlinks in the text.